Structure and electrical properties in the K1/2Bi1/2TiO3-K1/2Bi1/2ZrO3 solid solution (KBT-KBZ)

M. Bengagi, François Morini, M. El Maaoui, Pascal Marchet

Structure and electrical properties in the $K_{1/2}Bi_{1/2}TiO_3$ – $K_{1/2}Bi_{1/2}ZrO_3$ solid solution (KBT-KBZ)

M. Bengagi[1, 2], F. Morini[1,3], M. El Maaoui[2], P. Marchet[1,*]

[1] Laboratoire de Science des Procédés Céramiques et de Traitements de Surface (SPCTS), UMR 7315 CNRS, Université de Limoges, Centre Européen de la Céramique, 12 Rue Atlantis, 87068 Limoges Cedex, France
[2] Laboratoire de Chimie Minérale Appliquée, Faculté des Sciences, Université de Tunis El Manar, Campus Universitaire, 2092 - El Manar Tunis, Tunisie
[3] Present Address: Institut d'Electronique de Microélectronique et des Nanotechnologies (IEMN) - UMR CNRS 8520- Cité Scientifique, Avenue Poincaré, BP 60069, 59652 Villeneuve d'Ascq Cedex France

* Corresponding author: e-mail pascal.marchet@unilim.fr, Phone: +33 587 502 373, Fax: +33 587 502 307

Keywords $K_{0.5}Bi_{0.5}TiO_3$, $K_{0.5}Bi_{0.5}ZrO_3$, lead-free perovskite materials; electroceramics; X-ray diffraction; piezoelectric properties

Abstract

The present work is devoted to the study of the Zr^{4+} / Ti^{4+} substitution in the $K_{1/2}Bi_{1/2}Ti_{(1-x)}Zr_xO_3$ solid solution (x = 0.0 to x = 1.0), based upon the $K1_{/2}Bi_{1/2}TiO_3$ (KBT) ferroelectric compound. The tetragonal distortion of KBT is suppressed by this substitution and lead to the cubic compound $K_{1/2}Bi_{1/2}ZrO_3$ (KBZ). These results agree with the values of the ionic radii of the Zr^{4+} and Ti^{4+} ions (r Ti^{4+} = 0.605 Å and r Zr^{4+} = 0.72 Å). Close to KBT ($x \leq 0.05$), the symmetry remains tetragonal. For higher values of x, the "a" lattice parameter (cubic indexing) follows the Vegard's law, thus confirming the formation of a solid solution. The transformation from tetragonal to cubic proceeds thru an intermediate pseudo-cubic symmetry ($0.1 \leq x < 0.5$), for which the X-ray diffraction peaks present small broadening and asymmetry. For $x \geq 0.5$ and up to the KBZ compound (a □ 4.158 Å), the samples are cubic but some extra peaks are also observed, indicating the occurrence of a secondary phase. The microstructures shows fine-grained ceramic samples for the first range, while for the KBZ rich range the grains are micrometer-sized and associated to very small grains of the secondary phase. Piezoelectricity is observed for the tetragonal and pseudo-cubic range, the substitution quickly reducing the piezoelectric properties. The measurement of the dielectric properties revealed close to KBT a dielectric anomaly probably associated to the tetragonal – cubic phase transition. For the pseudo-cubic and cubic range, a broad dielectric anomaly is observed around 300 °C, corresponding to a relaxor behavior.

1 Introduction

The perovskite compounds ABO_3 are one of the most common oxide structures. Thus they have been extensively studied, since they present a very large panel of interesting physical properties such as ferroelectricity and piezoelectricity [1-8], superconductivity [9-11], giant magneto-resistance [12-14]… The interest for such compounds was recently renewed since multiferroic properties were evidenced in such materials [15-17], as well as new peculiar ferroelectric properties at nanoscale [18, 19] or for thin films form [20] and new physical phenomena due to interface properties [21-23]. Concerning the piezoelectric properties, the industrially-used compounds mainly belongs to the PZT family, a solid solution of formula $PbZr_{(1-x)}Ti_xO_3$, because of their unequalled properties. Thus, a lot of studies were devoted since 60 years to the structure and the properties of $PbZrO_3$ (PZ), $PbTiO_3$ (PT) and PZT [4, 24-28].

Because of restrictions on the use of hazardous substances, lead-based piezoelectric materials are now only tolerated for piezoelectric devices [29]. Thus, new lead-free materials are actually highly investigated. Among the different available materials, Bi-based compounds such as $Na_{1/2}Bi_{1/2}TiO_3$ (NBT) and $K_{1/2}Bi_{1/2}TiO_3$ (KBT) present interesting dielectric and ferroelectric – piezoelectric properties [6-7, 30-32]. As for PZT, such properties can be easily modulated by binary or ternary solid-solution formation, such as NBT-KBT [33-35], NBT-$BaTiO_3$ [36], NBT-KBT-$BaTiO_3$ [37], NBT-KBT-$Li_{0.5}Bi_{0.5}TiO_3$ [38, 39], NBT-$SrTiO_3$ [40, 41], double substitutions like for NBT-$PbZrO_3$ [42], NBT-$BiScO_3$ [42], NBT-$BiFeO_3$ [42-44], NBT-KBT-$BiAlO_3$ [45] or more complex substitution in A-site [46]. Some of these substitutions improve the piezoelectric properties of NBT and KBT, while some of them suppress the ferroelectricity, inducing sometimes interesting dielectric properties and/or relaxor behaviour. Thus, as for the PZT, the understanding of the relationships between structure and electrical properties is necessary, in order to be able to modulate and control the properties of the compounds before using them in devices.

At the present time, most of the studies concern the substitutions in the A-site of the perovskite lattice. But up to date, very few studies concern the substitution in B-site alone. Like for PZT, Zr^{4+} ion would logically replace Ti^{4+} in B-site. In order to test for this substitution, we selected the compound $K_{1/2}Bi_{1/2}TiO_3$ (KBT), a ferroelectric compound [10] of tetragonal symmetry (space group P4mm [a = 3.994 Å, c = 4.038 Å [47, 48]). The tolerance factor of KBT is larger than one ($t \approx 1.03$) and thus implies structural distortion by displacement of cations, like in $BaTiO_3$ ($t \approx 1.06$) and $PbTiO_3$ ($t \approx 1.02$), lone pair effect being observed in the last one (like for Bi^{3+} ion). As the ionic radius of the Zr^{4+} ion is larger than the one of Ti^{4+} (r Ti^{4+} = 0.605 Å and r Zr^{4+} = 0.72 Å for coordination number = 6 [49]), this structural distortion will decrease when substituting Zr^{4+} for Ti^{4+}. For the hypothetical compound $K_{1/2}Bi_{1/2}ZrO_3$ (KBZ), the calculated tolerance factor is smaller than unity ($t \approx 0.97$), thus similar to the one of $BaZrO_3$ ($t \approx 1.00$, cubic, space group P*m3m*) and of $PbZrO_3$ ($t \approx 0.96$, orthorhombic, space group P*bam*). Thus, a modifcation of structural distortion type can be predicted for the $K_{1/2}Bi_{1/2}Ti_{(1-x)}Zr_xO_3$ solid solution, the change probably occurring around $x \approx 0.5$ ($t \approx 1$). Furthermore, this substitution will also suppress the polar (ferroelectric) behaviour of KBT: a tolerance factor smaller than unity generally implies structural distortions by octahedra rotations, which are unfavourable to ferroelectricity, but lead more to antiferroelectric behaviour. Moreover, (i) the calculated tolerance factor lies between the ones of $BaZrO_3$ (paraelectric) and $PbZrO_3$ (antiferroelectric), and (ii) Pb^{2+} and (K^+/Bi^{3+}) pseudo-ion present similar ionic radii and lone pair effect (r Pb^{2+} = 1.49 Å and r K^+/Bi^{3+} = 1.51 Å for coordination number = 12 [49]).

At the present time, very few data are available for the KBZ compound or the KBT-KBZ solid solution. Smolenski reported in 1967 for the possible existence of KBZ [50]. A cubic-like X-ray diffraction pattern was published in 1985 [51] and a JCPDS/PDF card based upon this report was assigned to this compound [52]. But considering the tolerance factor calculated for KBZ, the real structure probably corresponds to distortion by octahedron tilting and thus to a non-cubic unit cell [53]. Concerning the $K_{1/2}Bi_{1/2}Ti_{(1-x)}Zr_xO_3$ system (KBT-KBZ), a continuous solid-solution was reported in a short study mainly dedicated to the dielectric properties [54]. A symmetry change from tetragonal to rhomboedral was also reported for $x \approx 0.1$, with a very small rhomboedral distortion (δ_r < 10 min angle).

Thus, the published results are ambiguous concerning both the hypothetical KBZ compound and the KBT-KBZ solid-solution. As a consequence, the aim of the present study is: (i) to confirm for the possibility of the Zr/Ti substitution in the $K_{1/2}Bi_{1/2}Ti_{(1-x)}Zr_xO_3$ solid solution. (ii) to verify for the existence of the $K_{1/2}Bi_{1/2}ZrO_3$ compound and (iii) to measure the dielectric and piezoelectric properties of such materials.

2 Experimental procedure

All the samples were elaborated by solid state reaction using ZrO_2 (Sigma-Aldrich 99.99%), TiO_2 (Sigma-Aldrich 99.8%), KNO_3 (Ventron > 99%) and Bi_2O_3 (Sigma-Aldrich 99.9%). The ZrO_2 and TiO_2 raw materials were first separately ball-milled in ethanol for two hours at 390-400 rpm using agate balls in an agate container (planetary mill "pulverisette", Fritsch, Idar-Oberstein, Germany), in order to reduce their mean particle sizes. They were then dried at 200 °C in order to suppress any residual water. After drying, these precursors were weighted according to the desired composition and homogenized by ball-milling in ethanol for two hours at 390-400 rpm. The obtained powders were then calcined at 900°C for 4 hours, milled again and annealed between 900 and 1000°C for 4 hours (x = 0.4 to x = 1), while this second calcination was performed for 10 hours for the Ti rich range (x = 0 to x = 0.3). On order to determine the best calcination temperatures, simultaneous thermogravimetric and thermal analysis (TG /DSC Netzsch STA 409, Selb , Germany) was ^performed on the initial mix of raw powders for different compositions using 10°C/mn heating rate. After calcination, the obtained powders were studied by X-ray diffraction (Bruker D8, θ/2θ configuration, LinxEye high speed detector, Cu $K\alpha_1$ radiation, step size 0.08°, Bruker AXS, Karlsruhe, Germany). The powders were then pressed into 10 mm diameter disks (≈ 43 MPa) and sintered at 1000 -1070°C for one hour. The obtained pellets were then electroded using platinum paint sintered at 800 °C for half an hour. The electrical characterizations were performed on these pellets using an impedance analyzer (HP 4194A, Agilent technologies, Santa Clara, California, USA) at several frequencies between 100 Hz and 1 MHz. Piezoelectric properties were evaluated, after a poling process. This one was carried out in a silicone oil bath at room temperature using a 10 kV DC high voltage source (SL10,

Spellman, New York, USA). The piezoelectric constant d_{33} was measured using a piezo–d33 meter (PM 300, Piezotest, London, UK). Field-emission scanning electron microscopy (FE-SEM, JEOL JSM-7400F) was employed for microstructural characterization on fractured samples coated with carbon. The average grain size was determined for grains presenting suitable contrast by using image processing. For each sample, More than 50 grains were selected and used for the calculation of equivalent diameters.

3 Results and discussion

3.1 Thermal analysis of the precursors

In order to determine the best calcination temperatures, simultaneous TG / DSC measurement was performed on the initial mix of raw powders corresponding to the KBT composition (fig.1). Similar results were obtained for compositions containing zirconium. Four endothermic events were evidenced by DTA. The first one corresponds to the polymorphic transformation α $KNO_3 \leftrightarrow \beta$ KNO_3 (128 °C) and the second one to the melting of KNO_3 (334 °C) [55]. The third event, quite large and diffuse, is associated to the progressive decomposition of liquid KNO_3. The last event corresponds to the transformation α $Bi_2O_3 \rightarrow \delta$ Bi_2O_3, which occurs at ≈ 730 °C [56]. Thus, the reaction between the different precursors implies a liquid phase. The measured weight loss (11%) corresponds well to the calculated one (10.9%) and are totally achieved above 800 °C. Thus, we selected 900 °C for the synthesis of the samples.

3.2 X-ray diffraction

The structural evolution was studied after calcinations of the powders, for compositions ranging from x = 0.0 to x = 1.0 (fig. 2). Whatever the composition, the main peaks of the pseudo-cubic cell are shifted to lower angles with KBZ substitution, indicating an increase of the mean pseudo-cubic lattice parameter, and thus the formation of a solid-solution. Contrary to previous report [54], we did not observe any evidence for rhomboedral symmetry for x > 0.1.

3.2.1 The KBT rich-range

For the KBT rich range ($0.0 < x \leq 0.4$), all the diffraction peaks are broad, which implies a chemical disorder. The diffraction patterns appear as quite complicated (fig. 2). The (111) pseudo-cubic peak is splitted into two peak (labelled A and B, fig. 2.b) and the angular position of these two peaks remains quasi constant from x = 0.05 to x = 0.2. The (200) pseudo-cubic peak is splitted into two or three peaks (labelled C and D, fig 2.b). Again, the angular position of these peaks remains quasi constant from x = 0.05 to x = 0.2. All these peaks can be attributed to two different perovskite structures P1 and P2, corresponding respectively to peaks A and C for P1 and to peaks B and D for P2.

The intensities of the peaks corresponding to perovskite P1 and P2 changes in reverse order, indicating that the content in P1 increase with x values, while P2 content decrease. Considering the angular position on the corresponding peaks and thus the mean pseudo-cubic lattice parameter, P1 and P2 have different Zr/Ti ratio, P2 containing less zirconium than P1. The same phenomena are also observed for the other peaks of the perovskite structure in the same composition range.

A similar behaviour has been previously reported for the solid solution $BaTiO_3$ –$BaZrO_3$ (BT – BZ) [57]: during synthesis of $BaTi_{0.6}Zr_{0.4}O_3$ (BTZ), BT and BZ form separately and then the BTZ solid solution appears by interdiffusion between BT and BZ: the formation of BTZ is limited by the diffusion of Ti-ion into BZ lattice. Thus, the X-ray diffraction patterns for powders calcined at low temperatures (900-1400°C) corresponds to the occurrence of two perovskite phases with different lattice parameters, as observed for our samples.

For the KBT-KBZ, the corresponding powders ($0.0 \leq x \leq 0.4$) appear similarly as being out of equilibrium: the chemical reaction between the different precursors is not fully achieved. As a consequence, we tried to complete the chemical reaction by performing annealing of the powders. For example, the X-ray diffraction diagrams of the x = 0.10 composition obtained for different annealing times is represented fig. 3 (samples from the same initial batch: one star for the first sample successively annealed three times for ten hours, two stars is for the second sample directly annealed for 50h two times). The results clearly demonstrate a structural evolution (fig.3.b): the “cubic” phase, associated to the most intense (200) peak progressively disappeared, while the (002) and (200) tetragonal peaks merged into a single (200) pseudo-cubic peak. This evolution corresponds to the chemical homogenization of the sample and can be explained by considering that the powder is initially composed of two perovskite structures with different chemical compositions (different Ti/Zr ratio), which evolves with annealing time toward a homogeneous pseudo-cubic structure. A similar behaviour was also observed for samples with $0.05 \leq x \leq 0$ 4 (fig. 4). For x = 0.05, the final symmetry was determined as being tetragonal with very small distortion. For the other compositions, the final symmetry appeared as pseudo-cubic, the departure from cubic symmetry appearing only as an asymmetry of the diffraction peaks (fig. 4.b). As we will see hereafter, this departure from "pure" cubic symmetry can explain the piezoelectric properties observed for these compositions.

As Bi-containing compounds such as NBT and KBT are prone to loss of volatile elements (Bi, Na, K) and as long dwell times at temperatures up to 1000°C could imply volatilization, the powders were systematically

weighed before and after annealing. Under the sensitivity of these measurements, no weight loss was observed. However, a small deviation from nominal composition can't be excluded, which could explain the occurrence of secondary phases for long annealing times.

3.2.3 Evolution of the lattice parameters

As a consequence of the previous observations, the lattice parameters were calculated for annealed powders close to KBT ($0 \leq x \leq 0.3$) and for raw powders for higher values of x. For pure KBT (fig.5), the refined peak profile function did not allow to obtain a perfect agreement between observed and calculated values, because of the asymmetry of some reflexions. However, the calculated values (a = 3.9247 Å, c = 3.9963 Å, c/a = 1.02) agree quite well with the reported values (a = 3.9388 Å, c = 3.9613 Å, c/a = 1.006) [47, 48]. The x = 0.05 sample also corresponds to a (small) tetragonal distortion similar to the one of pure KBT (P4mm).

For x = 0.2 to x = 0.4 samples, which still present asymmetry of the diffraction peaks after annealing, the refinement was performed twice, using either the cubic (Pm3m) or the tetragonal (P4mm) symmetry of KBT. As the tetragonal splitting (if existing) appears as very small, the corresponding samples were finally considered as being pseudo-cubic, the observed asymmetry being attributed more to a remaining chemical disorder than to a true tetragonal distortion. For the KBZ rich range ($x \geq 0.5$), this asymmetry is no more observed and the refinement was performed using a cubic cell (Pm3m).

For the KBZ compound, the X-ray diffraction diagram (fig.6) corresponds to a cubic perovskite structure, with lattice parameter a = 4.1582 Å, similar to the value previously reported (a = 4.1572 Å, [52]). Only small differences are observed compared to the JCDS card [52]: (i) the (100) peak is observed here, while it was not reported and (ii) some of the intensities present small differences for high Miller indices. A careful examination of the background revealed that some extra peaks are also observed, probably associated to a secondary phase. These peaks were also observed, with lower intensity, for the samples corresponding to $0.4 \leq x \leq 1$. Some of them could be assigned to monoclinic ZrO_2, one of our precursors, but all of them could not be totally attributed. Our attempts to eliminate this phase by annealing of the sample with intermediate grinding, or by introducing a K and Bi excess, were unsuccessful. We also used the process reported in [51] corresponding to the JCPDS card: heating a stoichiometric mixture of oxides and carbonates at 1100°C for 4 hours and 1200°C for 8 hours in a closed platinum crucible; but the result was the same. Thus, the identification of this secondary phase is not possible at the present time the K_2O-Bi_2O_3-ZrO_2 phase diagram being only partly known.

Finally, the evolution of the lattice parameters as a function of the composition indicates an increase of the mean pseudo-cubic lattice parameter, according to the values of the ionic radii (fig.7). The evolution observed follows Vegard's law, confirming the formation of a solid solution.

3.3 Ceramic sintering, electrical properties

3.3.1 Densification and microstructures

In order to study the electrical properties of these materials, sintering was performed as described above in the experimental procedure. As for other alkali-containing compounds such as $K_{0.5}Na_{0.5}NbO_3$, [58-60], the sintering appears as difficult, especially for Zr-rich samples (table 1). Thus, the electrical properties must take into account the low densities of some of the samples, since dielectric measurements generally require density values over 95%.

For the KBT rich range ($0 \leq x \leq 0.40$), the microstructure appears as being composed of nanometer-sized grains (300 – 500 nm) with fine rounded shape (fig.8), excepting for x = 0.1 and x = 0.3 for which the grain size appears as higher, may be because of a shorter milling time before sintering. However, for higher KBZ content ($0.50 \leq x \leq 1.00$), the morphology shows faceted grains with rounded corners, with larger size (2-5 µm). The microstructure presents also some porosity, according to the density values.

This difference in sizes and grain shapes suggests a modification of the sintering mechanism for KBZ-rich samples, the zirconium substitution inducing faster grain growth and thus increased porosity.

In addition, an intergranular phase is also observed, particularly for the KBZ-rich range, with very small grain size around 10-20 nm. This phase can be probably attributed to the unidentified secondary phase observed for these compositions by X-ray diffraction.

As a structural evolution occurred during annealing of some the initial powders, we suspected that a similar phenomenon could occur during sintering. Thus some of the samples were checked by X-ray diffraction (x = 0.5, x = 0.8 and x = 1.0). No difference was detected in the X-ray diffraction patterns before and after sintering.

3.3.2 Piezoelectric properties

The poling process was performed for all the samples. Poled ceramics were obtained for $0 \leq x \leq 0.4$ using $E \approx 3.5$-4 kV/mm for x = 0 (coercive field of KBT is reported as 3.5 kV/mm [61]), and $E \approx 2$ kV/mm for the others samples. Attempts to increase the applied field did not increase the measured d_{33} value. But we did not succeed

in poling any of the other samples (electrical breakdown occurred). The measurement of the ferroelectric cycles was also unsuccessful because of high conductivity, even for the samples which appeared as being piezoelectric after poling.

According to the structural observations indicating a tetragonally-distorted structure for x = 0.05 and a pseudo-cubic structure for x = 0.1 to x = 0.4, the piezoelectric coefficient d_{33} (fig.9) rapidly decreases with increasing x values, up to 2.4 pC/N for x = 0.1, then remains quasi constant up to x = 0.3 and vanishes for x = 0.4 (d_{33} = 0.3 pC/N, i.e. lower than the instrumental error estimated to ± 1 pC/N). These results agree well with the structural evolution determined by X-ray diffraction: like KBT, the x = 0.05 sample is tetragonal (with very small distortion), thus piezoelectric. For $0.1 \leq x \leq 0.4$, the samples appears as pseudo-cubic, the departure from pure cubic symmetry appearing only as an asymmetry of the diffraction peaks. Since these samples are not purely cubic, obtaining piezoelectricity is not surprising.

However, the piezoelectric constant values obtained for x = 0.1 to x = 0.4 are small, (d_{33} = 2.4 pC/N for x = 0.1 and d_{33} = 0.3 pC/N for x = 0.4). Finally, obtaining piezoelectricity for x = 0.4, but with a very small piezoelectric response, confirms that this composition is not truly cubic, even if we did not detect obvious structural distortion by X-ray diffraction. This fact also indicates that for higher values of x, the piezoelectric properties are suppressed by the substitution and that the corresponding compositions are centrosymmetric, as observed by X-ray diffraction.

3.3.3 Dielectric properties

The relative permittivity and dielectric losses were measured as a function of the temperature and frequency for some of the samples (fig. 10 and 11). The analysis of the electrical properties must take into account the low densities of some of the samples, since dielectric measurements generally require density values over 95%. Indeed, some of the samples present densities lower than 90%.

The values of tan(δ) are high and increase quickly above 300°C, indicating high conductivity. Thus, the apparent increase of permittivity above 400 – 500°C (especially for low frequency) is correlated to conductivity. Generally, high conductivity for dielectric materials can have two different origins: (i) a lack of densification, (ii) a micro structural effect and (iii) the occurrence of structural defects like vacancies. For the KBT rich range of this solid solution, the densification is over 95%. Thus, the origin of conductivity must be here more related with the occurrence of vacancies. Indeed, potassium and bismuth are known as being volatiles and losses of such chemical elements during sintering would create defects. For the KBZ rich range, which presents low densification, such conductivity phenomena are probably much more correlated the lack of densification.

Concerning the relative permittivity and as for previously published results [54], a broad anomaly is observed, with a maximum around ≈ 300°C, which is higher than previously reported for this system (150 – 200°C).

This maximum can be attributed to the tetragonal – cubic phase transition only close to KBT, since the x = 0.05 sample appears as tetragonal, but the other compositions present a pseudo cubic symmetry up to x = 0.4 and a thru cubic symmetry for $0.5 \leq x \leq 1$. In addition, this anomaly is frequency dependent (see tan(δ) curves) and thus clearly associated to a relaxor behaviour.

Indeed, such behaviour is characterized by the occurrence of a very broad ε(T) peak (or ε'(T) in complex notation of relative permittivity) and a strong frequency dispersion in the peak temperature (T_m) and in the magnitude of ε' below T_m [62]. This anomaly can also be observed in the tan(δ) (or ε") curves, the temperature for the maximum in ε' appearing always higher than in ε" (or tan(δ)) curves. The absence of obvious phase transition associated to these anomalies is also generally one of the representative features of relaxor materials [63].

As it is well known for the "model" relaxor, $PbMg_{1/3}Nb_{2/3}O_3$ (PMN), such behaviour is due to the occurrence of polar nano-regions (PNRs), which induces random-site electric dipoles, and the breadth of the ε'(T) peak is a manifestation of the dipolar glass-like response of these materials [62]. If the relaxor nature of NBT and KBT materials is known for a long time and widely accepted, their origin was still controversial up to recent times. Indeed, NBT presents a long-range ferroelectric order at room temperature, but at the so-called depolarization temperature (T_d ≈ 220°C), relaxor behaviour was observed, together with a broad maximum in the ε(T) curve around ≈ 300°C, and an apparently antiferroelectric behaviour between these two temperatures. Recent studies have clearly demonstrated for NBT, and thus probably also for KBT, that the dielectric anomalies have their origin in the occurrence of PNRs: The peculiar temperature T_d of NBT (and thus also for KBT), where the ferroelectric order disappears, is the temperature for which long-range ferroelectric order reverts back to relaxor state upon heating [64]. The behaviour of these materials is thus clearly of relaxor type, with a long-range ferroelectric order established at room temperature for NBT and KBT.

As for other complex perovskite materials, the occurrence of a relaxor behaviour for the KBT-KBZ solid solution is thus not surprising and can be considered as a consequence of the mixed occupation of A and B-sites [65]. Indeed, for NBT and KBT, A-sites are occupied both by Bi^{3+} and by an alkaline ion (Na^+, K^+). The mixed A-site occupation is thus responsible for their relaxor behaviour.

In addition, a ferroelectric/relaxor crossover can also be observed when compositional disorder is introduced by chemical substitutions [66] in ferroelectric materials, the behaviour changing from 'pure" ferroelectric to "pure" relaxor behaviour. Such phenomena have been observed for example for $BaTiO_3$-$BaZrO_3$-$CaTiO_3$ system, for which A-and B site substitutions are simultaneously introduced [67], and also for $Na_{0.5}Bi_{0.5}TiO_3$ based solid solutions with A and/or B-site substitution [33, 36, 41]: these chemical modifications generally induce an increase of the diffusivity of the phase transitions together with a relaxor behavior. Thus it is not surprising that the long-range ferroelectric order of KBT is suppressed by the Zr/Ti substitution and that the high chemical disorder induce relaxor behaviour.

Moreover, considering the general trend induced by Zr^{4+} content, the value of the relative permittivity at the maximum appears as decreased by KBZ substitution, together with a "flattening" of the curves. This evolution was expected on the basis of structural considerations: as the Zr^{4+} ion is larger than the Ti^{4+} one, the substitution implies a decrease of the off-centering of the B-ion in the BO_6 octahedron, thus destroying the ferroelectric behaviour and reducing the polar character of the cell. But this evolution must be considered carefully since these samples present low densities and high dielectric losses.

In addition, some of the samples also present a second peak, not frequency dependent ($T \approx 580$-600 °C). The origin of this anomaly is not totally known at the present time but it could be attributed to the secondary phase observed by X-ray diffraction.

3 Conclusions

In the present work, we studied for the possibility of substituting Zr^{4+} for Ti^{4+} in B-site of the $K_{1/2}Bi_{1/2}TiO_3$ perovskite compound. The X-ray diffraction results demonstrated that the tetragonal symmetry of KBT is observed only for low Zr content ($x = 0.05$). For higher values of x, the tetragonal distortion of KBT is suppressed and a cubic symmetry is observed for the zirconium-rich part of the $K_{1/2}Bi_{1/2}Ti_{(1-x)}Zr_xO_3$ solid solution ($x > 0.5$).

For the range corresponding to the transition between these two symmetries ($0.1 \leq x < 0.5$), the powders obtained directly after chemical reaction were structurally disordered and appeared as a mix of two perovskite phases with different compositions an symmetry. By annealing, we evidenced for an evolution toward a pseudo cubic symmetry: the calculation of the lattice parameters using a tetragonal lattice showed that, if present, this distortion is very small.

For the pseudo cubic and cubic range, ($x = 0.1$ to $x = 1.0$), the "a" lattice parameter increase with x values, according to the ionic radius of the Zr^{4+} ion, larger than the Ti^{4+} one. A "quasi perfect" Vegard's law is observed.

For the tetragonal and pseudo cubic ranges, piezoelectric properties were detected with a rapid decrease of d_{33} coefficient induced by the substitution.

Finally, the dielectric properties were measured. For low values of x (tetragonal range, $x = 0.05$), a dielectric anomaly associated to the tetragonal – cubic phase transition of KBT is observed. For higher values of x, a broad dielectric anomaly is observed around 300 °C, which corresponds to relaxor behaviour. Further experiments are now in progress in order to try to reduce conductivity by optimization of the sintering temperature and dwell time.

References

[1]. B. Wul, Nature **157**, 808 (1946)
[2] G. Shirane, S. Hoshino, K. Suzuki, J. Phys. Soc. Japan, 5, 453-455 (1950)
[3] G.A. Smolenskii, Zh. Rekhn. Fiz. 20 (1950), 137-148; Dokl. Akad. Nauk SSSR, 70, 405-408 (1950)
[4] B. Jaffe, W.R. Cook, H. Jaffe, Piezoelectric Ceramics (American Press, London and New York, 1971)
[5] N. Ramadass, Mat. Sci. Eng., 36, 231-239 (1978)
[6] T. Takenaka, K. Maruyama, K. Sakata, Jpn. J. Appl. Phys. 30, 2236-2239 (1991)
[7] T. Takenaka, H. Nagata, J. Europ. Ceram. Soc. 25 (2005)
[8] J.F. Scott, Science, 315, 954-959 (2007)
[9] J. G. Bednorz, K.A. Muller, Z. Phys. B Cond. Matt. 64, 189-193 (1986)
[10] J. G. Bednorz, K.A. Muller, M. Takashige, Science **236**, 73-75 (1987)
[11] M.K. Wu, J.R. Ashburn, C.J. Torng, P.H. Hor, R.L. Meng, L. Gao, Z.J. Huang, Y.Q. Wang, C.W. Chu, Phys. Rev. Lett. 58, 908–910, (1987)
[12] T. Tokura, U. Urushibara, Y. Moritomo, A. Asamitsu, Y. Tomioka, T. Arima, G. Kido, Mat. Sci. Eng. B, 31, 187-191 (1995)
[13] R; Mahendiran, R. Mahesh, A.K. Raychaudhuri, C.N.R. Rao, Pramana, 44, L393-L396, (1995)
[14] A. Maignan, C. Simon, V. Caignaert, B. Raveau, Solid Stat. Comm.96, 623-625 (1995)
[15] J. Wang, J.B. Neaton, H. Zheng, V. Nagarajan, S.B. Ogale, B. Liu, D. Viehland, V. Vaithyanathan, D.G. Schlom, U.V. Waghmare, N.A. Spaldin, K.M. Rabe, M. Wuttig, R. Ramesh, Science, 299, 1719-1722 (2003)
[16] W. Prellier, M.P. Singh, P. Murugavel, J. Phys. Cond. Matt. 17, R803-R832 (2005)
[17] R. Ramesh, N.A. Spaldin, Nat. Mater. 6, 21-29 (2007)
[18] C.H. Ahn, K.M. Rabe, J.M. Triscone, Science, 303, 488-491 (2004)

[19] P.M Rorvik, T. Grande, M.A. Einarsrud, Adv. Mater. 23, 4007-4034 (2011)
[|20] N. Setter, D. Damjanovic, L. Eng, G. Fox, S. Gevorgian, S. Hong, A. Kingon, A. Kohlstedt, N.Y. Park, G.B. Stephenson, I. Stolitchnov, A.K. Tangastev, D.V. Taylor, T. Yamada, S. Streiffer, J. Appl. Phys., 100, 051606 (2006)
[21] A; Ohtomo, H.Y. Hwang, Nature, 427 (2004), 423-426
[22] B. Lui, X. Hu, Phys. Rev. B, 81, 144504 (2010)
[23] J. Biscaras, N. Bergeal, A. Kushwaha, T. Wolf, A. Rastogi, R.C. Budhani, J. Lesueur, Nature Comm., 1 (2010)
[24] B. Noheda, Curr. Opin. Solid St. M. **6**, 27-34 (2002)
[25] Michael J. Hoffmann, H. Kungl, Curr. Opin. Solid St. M. **8**, 51-57 (2004)
[26] D.C. Lupascu, J. Rodel, Adv. Eng. Mater. 7, 882-898 (2005)
[27] Nina Balke, Igor Bdikin, Sergei V. Kalinin and Andrei L. Kholkin, J. Am. Ceram. Soc. **92,** 1629–1647 (2009)
[28] N. Zhang, H. Yokota, A. M.Glazer and P. A. Thomas, Acta Crys. **B67**, 386-398 (2011)
[29] Directive 2002/95/EC, Official Journal of the European Union, **46** (L37), 19-23 (2003)
[30] S. Zhang, R. Xia, T. Shrout, J. Electroceram. **19**, 251–257 (2007)
[31] P.K. Panda, J. Mater. Sci. **44**, 5049-5062 (2009)
[32] J. Rodel, W. Jo, T.P. Seifert, E.M. Anton, T. Granzow, D. Damjanovic, J. Am. Ceram. Soc. **92**, 1153-1177 (2009)
[33] O. Elkechai, M. Manier, J.P. Mercurio, Phys. Status Solidi A, **157**, 499-506 (1996)
[34] V.A. Isupov, Ferroelec. **315**, 123-147 (2005)
[35] Y.M. Li, R.H. Liao, X.P Jiang, Y.P. Zhang, J. All. Compd. **484**, 961-965 (2009)
[36] J.R. Gomah-Pettry, P. Marchet, A. Simon, R. Von Der Muhll, M. Maglione, J.P. Mercurio, Int. Ferr. **61**, 155-158 (2004)
[37] Y.M. Li, W. Chen, Q. Xu, Xy Gu, Mat. Lett. **59**, 1361-1362 (2005)
[38] Y. Hiruma, K. Yoshii, H. Nagata, T. Takenaka, J. Appl. Phys. **103**, 084121 (2008)
[39] W. Lu, Y. Wang, G. Fan, X. Wang, F. Liang, J. All. Compd. **509**, 2738-2744 (2011)
[40] V.V. Bogatko, Y.N. Venevtsev, A.I. Abramova, Inorg. Mat. **16**, 72-74 (1980)
[41] J.R. Gomah-Pettry, A.N. Salak, P. Marchet, V.M. Ferreira, J.P. Mercurio, Phys. Status Solidi B, **241**, 1949-1956 (2004)
[42] P. Marchet, E. Boucher, V. Dorcet, J.P. Mercurio, J. Europ. Ceram. Soc. **26**, 3037-3041 (2006)
[43] V. Dorcet, P. Marchet, G. Trolliard, J. Europ. Ceram. Soc. **27**, 4371-4374 (2007)
[44] V. Dorcet, P. Marchet, G. Trolliard, J. Mag. Mag. Mat. **321**, 1762-1766 (2009)
[45] A. Ullah, C.W. Ahn, I. Won Kim, Phys. Status Solidi A **307**, 2578-2584 (2010)
[46] D. Lin, D. Xiao, J. Zhu, P. Yu, Phys. Status Solidi A **202**, R89-R91 (2005)
[47] G. Jones, J. Kreisel, P.A. Thomas, Powder Diffr. **17,** 301-319 (2002)
[48] PDF card # 01 – 072-81210339 (JCPDS)
[49] R.D. Shannon, Acta Crys. **A32**, 751-767 (1976)
[50] G.A. Smolenski, N.N. Krainik, N.P. Khuchua, V.A. Isupov, V.V. Zhdanova, O.M. Mushtare, A.Y. Cherkash, Izv. Akad. Nauk. Fiz. (in Russian) **31**, 1164-1167 (1967)
[51] Y. Venetsev, E. Politova, S. Ivanov in "Ferro and Antiferroelectrics of barium titanate family" (Chemistry, Moscow, Russian Federation, 1985), p. 256 (in Russian)
[52] PDF card # 057-0823 (JCPDS)
[53] R.H. Mitchell, "Perovskites: modern and ancient" (Almaz Press, Canada, 2002)
[54] Y. Yamada, T. Akatsu, H. Asada, K. Nozawa, S. Hachiga, T. Kurosaki, O. Ikagawa, H. Fujiki, K. Hozumi, T. Kawamura, T. Amakawa, K. Hirota, T. Ikeda, Jpn. J. Appl. Phys. **34**, 5462-5466 (1995)
[55] A. Norlund Christensen, P. Norby, J.C. Hanson, S. Shimada, J. Appl. Crystallogr. **29**, 265-269 (1996)
[56] D. Risold, B. Hallstedt, L.J. Gauckler, S.G. Fries, J. Phase Equilib. **16**, 223-234 (1995)
[57] J. Bera, S.K. Rout, Mat. Lett. **59**, 135-138 (2005)
[58] B.P. Zhang, L.M. Zhang, J.F. Li, H. Zhang, S. Jin, Mat. Sci. Forum, **475-479**, 1165-1168 (2005)
[59] J. Bernard, A. Bencan, T. Rojac, J. Holc, B. Malic, M. Kosec, J. Am. Ceram. Soc., **91**, 2409-2411 (2008)
[60] C.M. Cheng, M.C. Kuan, K.H. Chen, C.C. Shih, J.S. Jiang, Adv. Mat. Res. **239-242**, 994-997 (2011)
[61] K.Yoshii, Y. Hiruma, H. Nagata, T. Takenaka, Jpn. J. Appl. Phys. **45**, 4493-4496 (2006)
[62] G.A. Samara, J. Phys.: Condens. Matter. **15,** R367-R411 (2003)
[63] L.E. Cross, Ferroelectrics, **76**, 241-267 (1987)
[64] W. Jo, S. Schaab, E. Sapper, L.A. Schmitt, H.J. Kleebe, A.J. Bell, J. Rodel, J. Appl. Phys. **110**, 074106 (2011)
[65] R. Dittmer, W. Jo, J. Daniels, S. Schaab, J. Rodel, J. Am. Ceram. Soc. **94**, 4283-4290 (2011)
[66] G.A. Samara, E.L. Venturini, Phase Transit. **79**, 21-40 (2006)
[67] J. Ravez, C. Broustera, A. Simon, J. Mat. Chem. **9**, 1609-1613 (1999).

Table 1: relative densities of the ceramic samples (based upon the theoretical one calculated using cubic lattice parameters), mean equivalent diameters and standard deviations.

X value	0.00 (KBT)	0.05	0.10	0.20
Relative density (%)	93	94.3	98.6	97.2
Mean diameter (µm)	0.59 ± 0.09	/	1.3 ± 0.2	0.85 ± 0.25
X value	0.30	0.40	0.50	0.60
Relative density (%)	97.0	94.7	95	82
Mean diameter (µm)	1.8 ± 0.3	0.8 ± 0.3	1.9 ± 0.7	2.8 ± 0.8
X value	0.7	0.8	0.9	1
Relative density (%)	87	91	87	75
Mean diameter (µm)	2.5 ± 0.8	2.4 ± 0.8	2.0 ± 0.8	3.0 ± 1.4

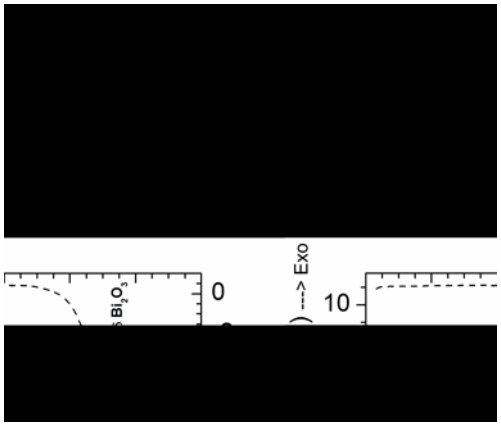

Figure 1 TG-ATD of the initial powder corresponding to the KBT composition

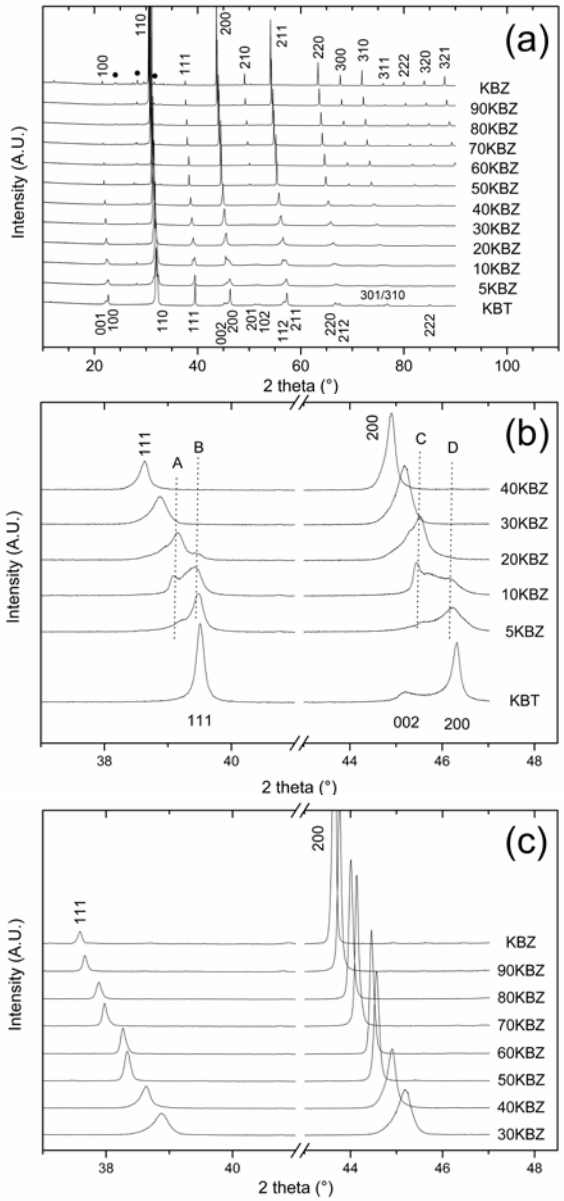

Figure 2 (a) X-ray diffraction diagrams of the $K_{1/2}Bi_{1/2}Ti_{(1-x)}Zr_xO_3$ compounds ($0 \leq x \leq 1$, circles = ZrO_2 secondary phase), and detail of the range corresponding to the (111) and (200) peaks (pseudo-cubic indexing for the solid-solution and tetragonal indexing for KBT), (b) $0 \leq x \leq 0.4$ and (c) $0.3 \leq x \leq 1$.

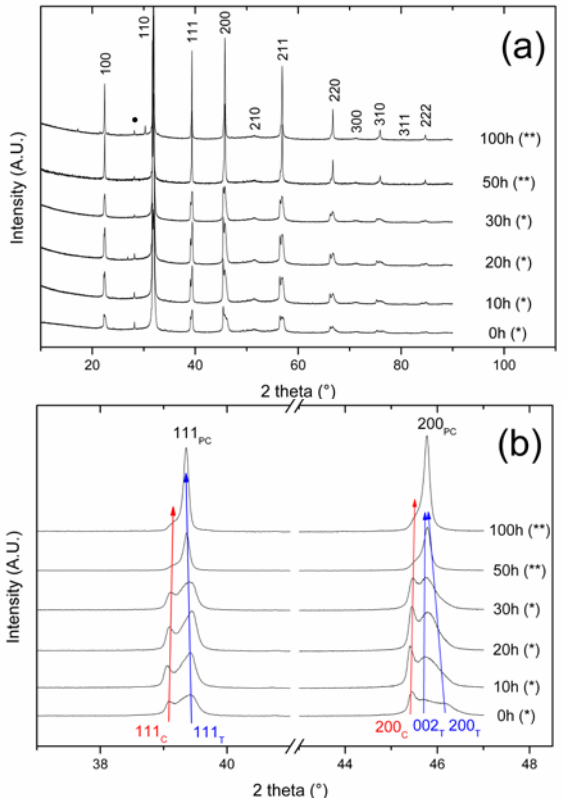

Figure 3 (a) X-ray diffraction diagrams of the $K_{1/2}Bi_{1/2}Ti_{0.90}Zr_{0.10}O_3$ composition for different annealing times. (★: samples annealed successively three times for 10h, ★★: same initial batch annealed directly two times for 50h).

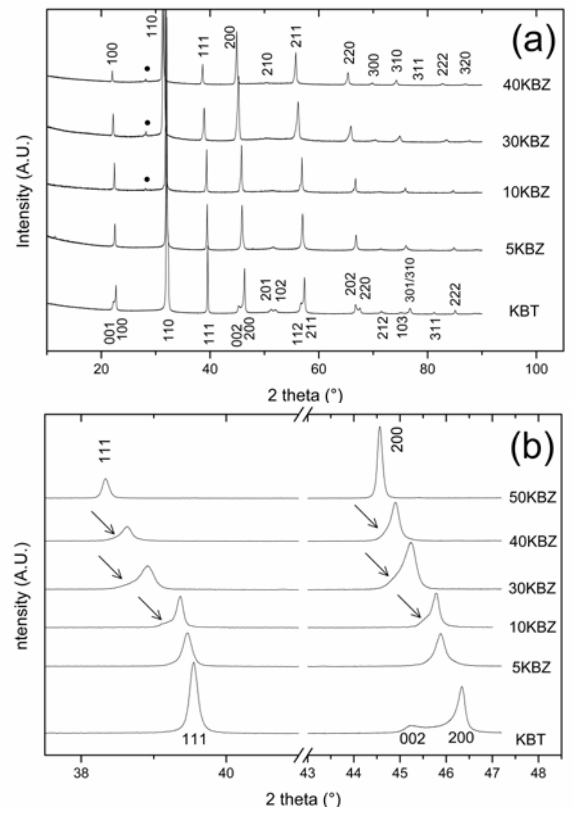

Figure 4 (a) X-ray diffraction diagrams of $K_{1/2}Bi_{1/2}Ti_{(1-x)}Zr_xO_3$ compounds (• = ZrO_2), (b) detail for the (111) and (200) peaks. The x = 0.05 and x = 0.1 were annealed at 1000°C for 50h, x = 0.3 at 1000°C for 10h, x = 0.4 and x = 0.5 are raw samples (The arrow shows the asymmetry indicating a departure from pure cubic symmetry).

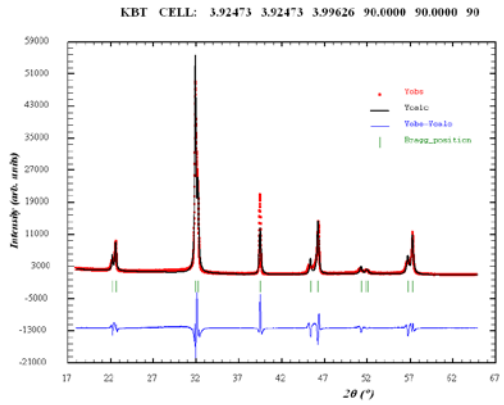

Figure 5 X-ray diffraction refinement diagram for the $K_{1/2}Bi_{1/2}TiO_3$ (KBT), compound.

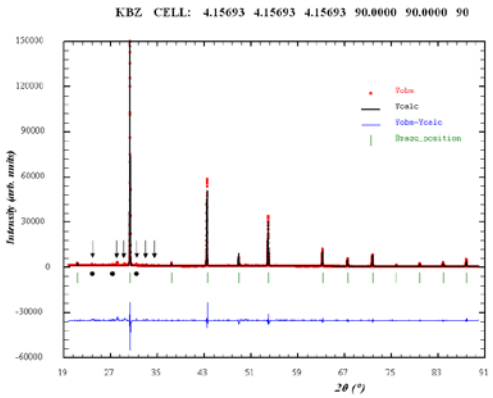

Figure 6 X-ray diffraction refinement diagram for the $K_{1/2}Bi_{1/2}ZrO_3$ (KBZ) compound (Circles correspond to ZrO_2 secondary phase, arrows correspond to unidentified phase).

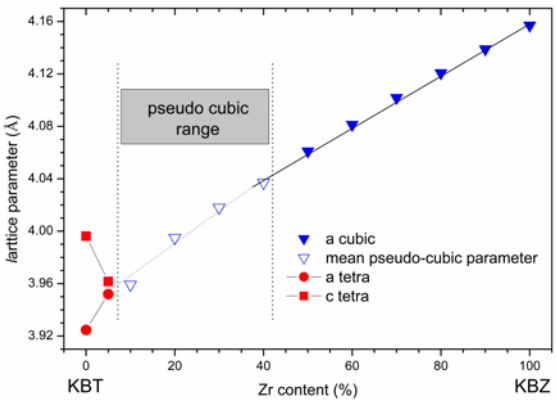

Figure 7 Evolution of the lattice parameters as a function of the composition for the $K_{1/2}Bi_{1/2}Ti_{(1-x)}Zr_xO_3$ compounds (standard deviation for the "a_c" parameter is ± 0.0005 Å and estimated to ± 0.005 Å for the pseudo-cubic range).

Composition	X 5000
X = 0 (KBT)	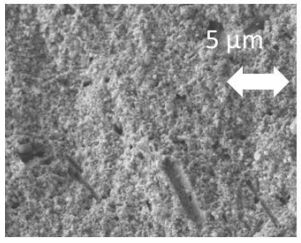
X = 0.10	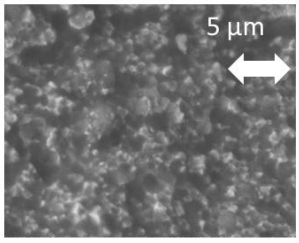
X = 0.20	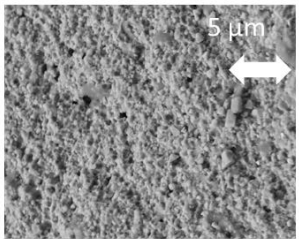
X = 0.30	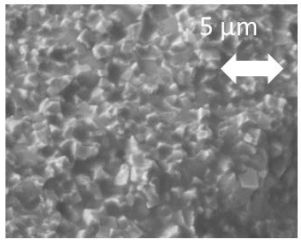
X = 0.40	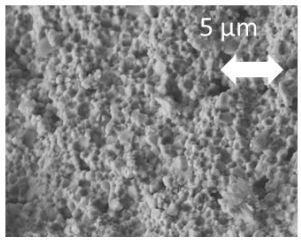
X = 0.50	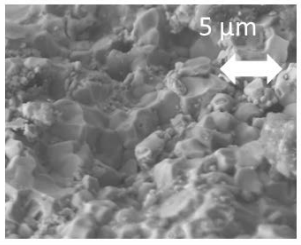

Composition	X 5000
X = 0.60	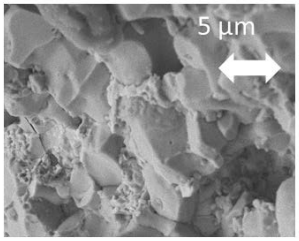
X = 0.70	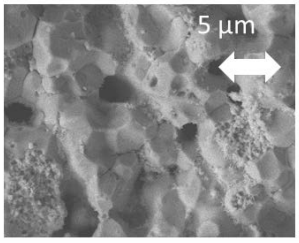
X = 0.80	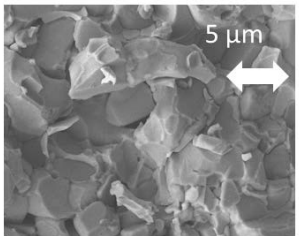
X = 0.90	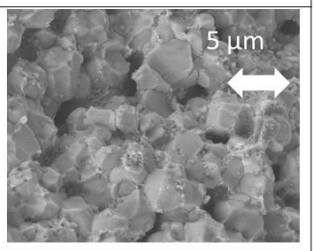
X = 1.00 (KBZ)	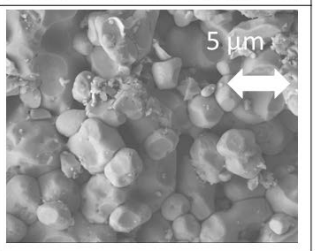

Figure 8. a SEM pictures of the ceramic samples (magnification 5000, $0 \leq x \leq 0.5$). (b) SEM pictures of the ceramic samples (magnification 5000, $0.6 \leq x \leq 1.0$).

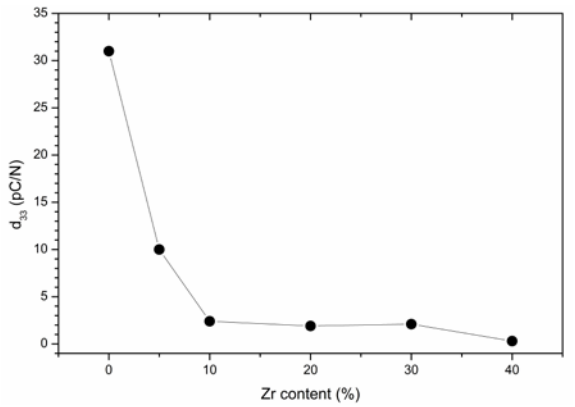

Figure 9 Evolution of the piezoelectric coefficient as a function of the composition.

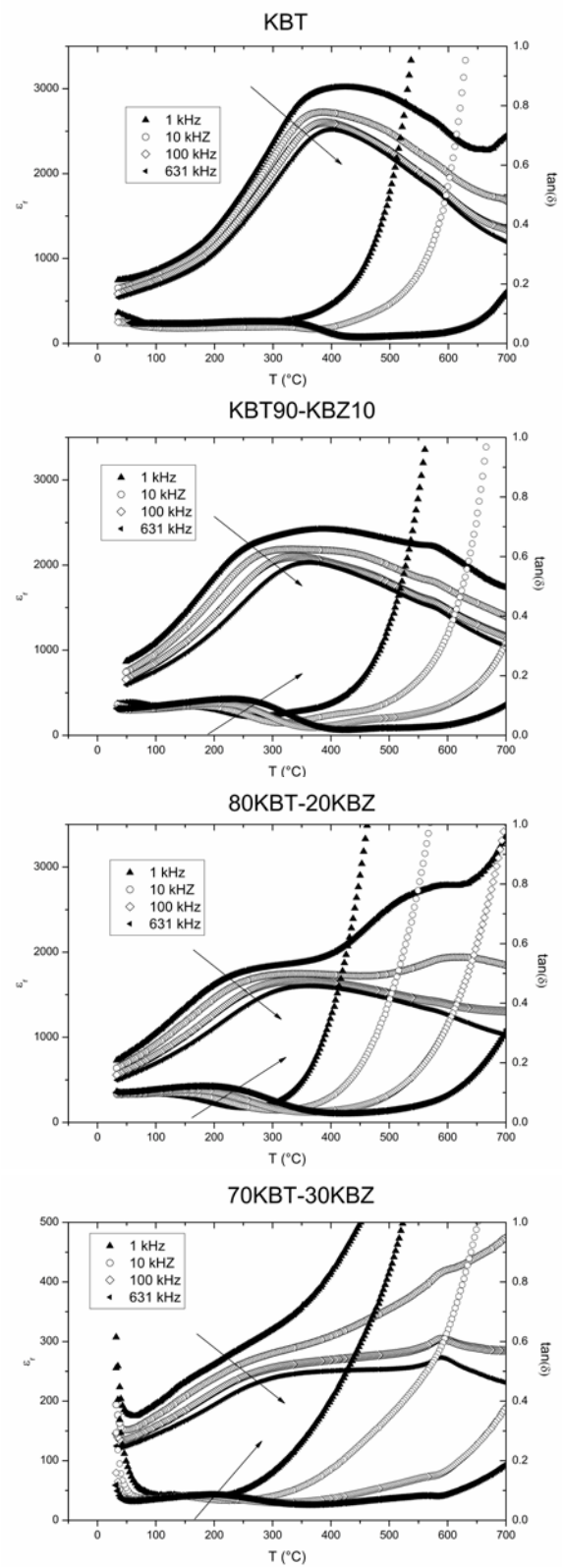

Figure 10 Dielectric properties of the $K_{1/2}Bi_{1/2}Ti_{(1-x)}Zr_xO3$ compounds as a function of the temperature for the KBT rich range (arrows indicate increasing frequencies).

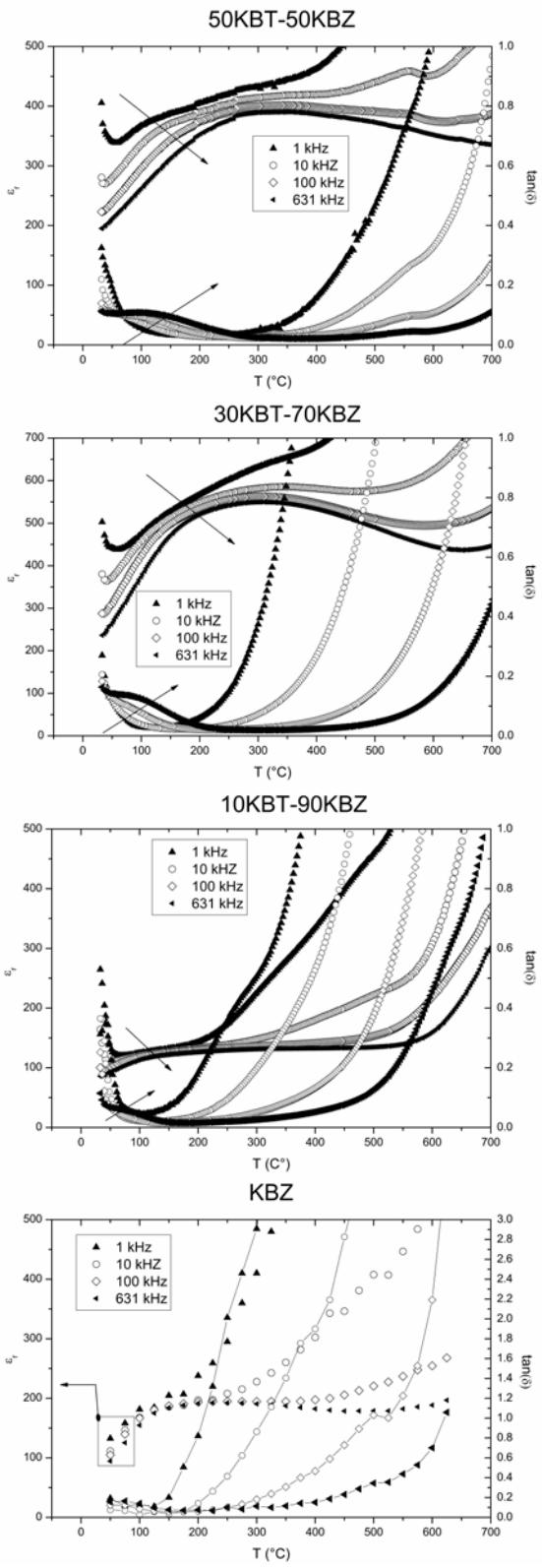

Figure 11 Dielectric properties of the $K_{1/2}Bi_{1/2}Ti_{(1-x)}Zr_xO_3$ compounds as a function of the temperature for the KBZ rich range (arrows = increasing frequencies; the KBZ composition was measured differently because of a controlling computer problem).